RESEARCH ARTICLE

VOLCANICA

Fast or slow: An evaluation of Ti-in-quartz diffusion coefficients through comparisons of quartz and plagioclase diffusion times

Sophia Y. Wang*[α,β], Guilherme A. R. Gualda[α], Jordan Lubbers[ϒ], and Adam J. R. Kent[β]

[α]Department of Earth and Environmental Sciences, Vanderbilt University, Nashville, TN, USA.
[β]College of Earth, Ocean, and Atmospheric Sciences, Oregon State University, Corvallis, OR, USA.
[ϒ]U.S. Geological Survey, Alaska Volcano Observatory, Anchorage, AK, USA.

Submitted: 2024-05-31 | Accepted: 2025-02-28 | Published: 2025-04-05

Editor: J. Farquharson | Typesetter: J. Farquharson

Abstract

Diffusion geochronometry using Ti-in-quartz has become a valuable method in understanding the evolution of silicic magmas. However, four different options for Ti diffusivity (D_{Ti}) currently exist, spanning three orders of magnitude, resulting in substantially different estimated times and interpretations. We present Ti-in-quartz diffusion times for the Cerro Galán Ignimbrite using the Cherniak et al. [2007] (10.1016/j.chemgeo.2006.09.001), Audétat et al. [2021] (10.1130/g48785.1), Audétat et al. [2023] (10.1038/s41467-023-39912-5), and Jollands et al. [2020] (10.1130/g47238.1) D_{Ti} value and (1) compare these against plagioclase diffusion times derived from the same samples, (2) consider evidence for Ti diffusion in quartz under relevant magmatic timescales, and (3) compute derived quartz growth rates for crystals from the Cerro Galán Ignimbrite. On all accounts, we find that the Cherniak et al. [2007] diffusion coefficient yields diffusion times that agree much better with independent evidence than those derived using slower D_{Ti} values [Jollands et al. 2020; Audétat et al. 2021; 2023].

Non-technical summary

Volcanic eruptions pose significant hazards to society. It is critical for us to better understand how they work. Titanium-in-quartz diffusion geochronometry—whereby we use variations in Ti concentration in quartz to estimate the time quartz grains spend under magmatic temperatures—can be useful to assess the longevity of silicic magmas that feed eruptions to the surface. However, there are currently four different diffusion coefficients for titanium-in-quartz that yield drastically different diffusion times—from 1000 years to 1,000,000 years! To test which of these measured diffusion coefficients most closely match geological constraints, we calculate and compare quartz diffusion times using four different coefficients to (1) known plagioclase diffusion times from the same system, (2) expected levels of diffusion, and (3) expected quartz growth rates. We find that the faster diffusion coefficient—which yields diffusion times of ~1000 years for quartz from the Cerro Galán Ignimbrite—agrees best on all three accounts.

Keywords: Geochronometry; Diffusion; Ti-in-Quartz; Cerro Galán Ignimbrite; Diffusion timescales; Growth rates.

1 Introduction

Understanding magmatic evolution within subvolcanic magma plumbing systems is essential for understanding the processes that lead to volcanic eruptions [e.g. Cashman et al. 2017]; however, it is remarkably difficult to do so given our inability to directly observe magma bodies in the subsurface over their 100 to 1,000,000 year timescale of evolution [Jicha et al. 2006; Wilson and Charlier 2009; von Quadt et al. 2011]. Diffusion geochronometry of major or trace components in common mineral phases of large silicic magma systems, such as plagioclase, sanidine, and quartz, provide considerable insight on the magmatic timescales in shallow storage directly preceding eruptions [e.g. Wark et al. 2007; Gualda et al. 2012a; Matthews et al. 2012; Cooper and Kent 2014; Pamukçu et al. 2015; Till et al. 2015; Gualda and Sutton 2016; Seitz et al. 2016; Rubin et al. 2017; Gualda et al. 2018; Shamloo and Till 2019; Boro et al. 2021; Pitcher et al. 2021; Lubbers et al. 2022; 2024].

Diffusion geochronometry of felsic minerals in large silicic systems typically use the trace-element compositional disequilibria across mineral zones and Fick's 2nd Law [Fick 1995] to calculate the time in which that zone boundary has existed at magmatic conditions [Morgan et al. 2004; Costa et al. 2008; Gualda et al. 2012a; Costa et al. 2014; Costa et al. 2020].

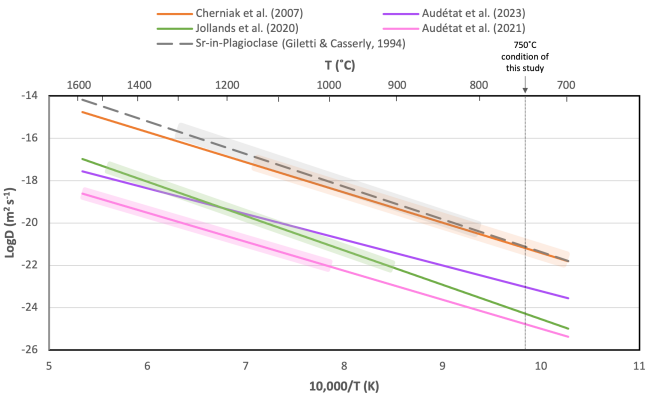

Figure 1: Arrhenius plot of the different Ti-in-quartz diffusion coefficients and the Sr-in-plagioclase diffusion coefficient. The four Ti-in-quartz coefficients are shown in colors and the Sr-in-plag coefficient [Giletti and Casserly 1994] is shown as a dashed grey line. Experimental ranges for each coefficient are highlighted respectively for relevant coefficients. The temperature condition of this study is outlined at 750 °C.

*✉ sophiawang.nz@gmail.com

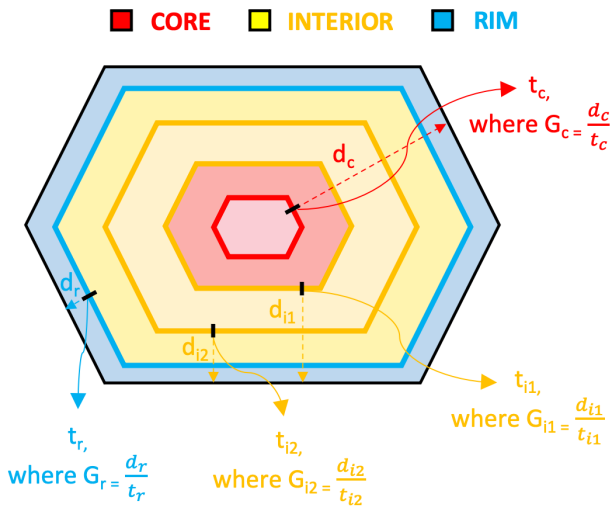

Figure 2: Schematic diagram of quartz zones and boundaries. Black lines indicate a measured zone boundary profile. Dashed arrows show minimum growth distance (*d*) from boundary of interest to the crystal rim. Curved arrows show location of maximum diffusion timescale (*t*) derived from boundary profile. Growth distance and diffusion timescale are then used to calculate minimum quartz growth rate (*G*). Colors represent core (red), interior (yellow) and rim (blue) regions. Measurements are derived from all regions and provide sequential information across the crystal.

This is done by determining (or assuming) the initial boundary profile, measuring the existing profile, and calculating the progression from initial state to current state as a function of time, resulting in a diffusion relaxation time. Titanium (Ti) is the dominant element used in diffusion geochronometry of quartz crystals in magmatic rocks [Wark et al. 2007; Gualda et al. 2012a; Matthews et al. 2012; Spear et al. 2012; Chamberlain et al. 2014; Pamukçu et al. 2015; Gualda and Sutton 2016]. Using the Ti diffusion coefficients (D_{Ti}) determined experimentally by Cherniak et al. [2007], diffusion times for intracrystalline boundaries typically yield values of 10^1–10^3 years [Gualda et al. 2012a; Matthews et al. 2012; Pamukçu et al. 2015; Gualda and Sutton 2016; Gualda et al. 2018; Cooper 2019; Costa et al. 2020; Pitcher et al. 2021]. However, new D_{Ti} have been proposed [Jollands et al. 2020; Audétat et al. 2021; 2023], which are one to three orders of magnitude smaller than the previous estimate (Figure 1) which, when directly applied to previous diffusion models, lead to much longer calculated times (10^3–10^7 years) of quartz residence at magmatic temperatures. Importantly, three of the four studies, including those that reach contrasting conclusions [Cherniak et al. 2007; Jollands et al. 2020; Audétat et al. 2021], use similar—though not identical—experimental setups. Accurately replicating geological conditions of kinetic processes is an outstanding challenge in experimental studies and thus has led to orders of magnitude differences in experimentally-defined D_{Ti}, leaving important implications for Ti-in-quartz geochronometry. In this work, we seek to test which of these D_{Ti} is most consistent with results obtained using natural samples that experienced diffusion under magmatic conditions. We do not seek to explain the source of the inconsistencies between the experimental studies, nor do we question the quality of science or data produced from them—rather, we pursue independent tests that can clarify which results are more likely to be consistent with natural magmatic systems and thus useful for Ti-in-quartz geochronometry.

Our study focuses on the Cerro Galán Ignimbrite [Francis et al. 1983; Sparks et al. 1985], using quartz from the same samples studied by Lubbers et al. [2022] to calculate multiple sets of Ti-in-quartz diffusion timescales for each D_{Ti}. These sets of diffusion times allow us to (1) compare our Ti-in-quartz geochronometry results for rims, interiors, and cores of quartz crystals (see Figure 2) using the different D_{Ti} against the results of plagioclase geochronometry obtained by Lubbers et al. [2022], (2) test whether diffusional relaxation of Ti compositional profiles in quartz takes place under magmatic conditions in the Cerro Galán Ignimbrite system by looking at diffusion trends from core to rim, and (3) calculate quartz growth rates based on each set of D_{Ti} diffusion times, and compare against independently determined growth rates [e.g. Pamukçu et al. 2015]. We present results using the Cherniak et al. [2007] coefficient ($D_{Ti}^{Cherniak}$), the Audétat et al. [2023] coefficient ($D_{Ti}^{Audétat23}$), and the Jollands et al. [2020] coefficient ($D_{Ti}^{Jollands}$). For simplicity we use the Jollands et al. [2020] coefficient as a representative of itself and the Audétat et al. [2021] coefficient, given that Jollands et al. [2020] originally sparked this discussion, and the two yield results on the same order of magnitude which, for the purposes of this study, lead to the same conclusions (see Figure 1) . Here, we define diffusion time as the amount of time that the mineral zone boundary of interest has existed in magmatic conditions (residence time at magmatic conditions), while crystallization or crystal growth refer to the initial formation of the given crystal or zone boundary.

2 Methods

We use 93 quartz crystals derived from 8 white pumice samples collected from various locations of Cerro Galán Ignimbrite (see Figure 1 of Lubbers et al. [2022]; also Folkes et al. [2011]). These quartz crystals were derived from the same 8 samples from which plagioclase crystals were derived from in Lubbers et al. [2022] and are mounted in polished epoxy mounts using the same preparation procedures as the plagioclase crystals. No effort was made to place quartz crystals in specific orientations during mounting given the nearly isotropic diffusion coefficient, at least as measured by Cherniak et al. [2007] .

2.1 CL imaging

Carbon-coated epoxy mounts containing the quartz crystals were imaged on a Tescan VEGA3 variable-pressure scanning electron microscope (SEM) installed in the Department of Earth & Environmental Sciences at Vanderbilt University. Imaging conditions include an accelerating voltage of 15 kV, working distance of ~15 mm, and a beam intensity of 17–19, such as to yield an absorbed current of approximately 2 nA [see Gualda and Sutton 2016]. The dwell times are

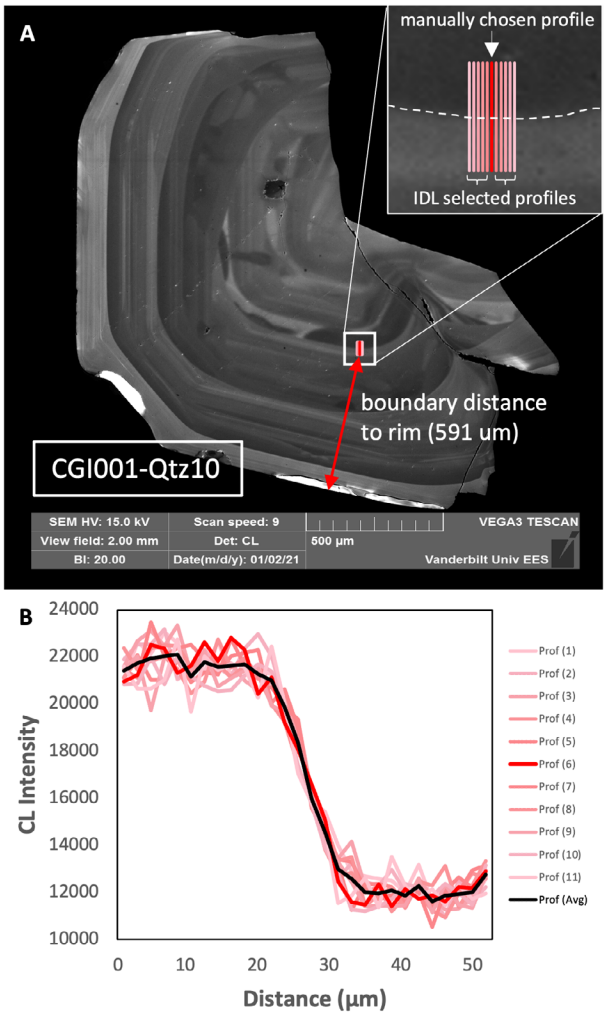

Figure 3: Illustration of strategy to select cathodoluminescence (CL) profiles from CL images for a boundary of interest. [A] CL image, with 11 profiles selected, while inset shows a detailed view. Using the program `'cl_profile'`, the user selects a profile of interest (dark red line), and the program selects an additional 5 profiles on each side (lighter red lines). [B] CL intensity (arbitrary unit) as a function of position (in µm) for the 11 profiles, as well as for the average profile (in black).

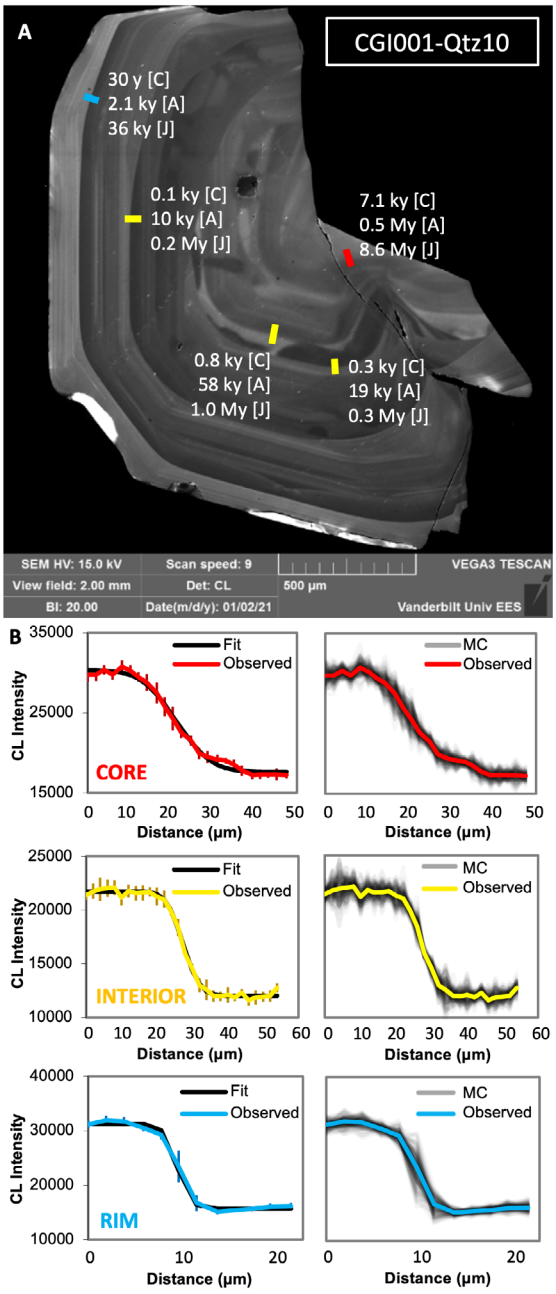

Figure 4: Example of Ti-in-quartz diffusion profiles for the Cerro Galán Ignimbrite. [A] Cathodoluminescence image showing zoning in quartz, with profiles labelled with the diffusion timescale estimated using the Cherniak et al. [2007] (labelled **[C]**), Audétat et al. [2023] (labelled **[A]**), and the Jollands et al. [2020] (labelled **[J]**) Ti-in-quartz diffusion coefficients. [B] Examples of retrieved CL profiles. Left column shows average diffusion profiles (colors) and their model fit (black), with error bars. Right column shows corresponding diagrams with the average profile and 200 synthetic profiles generated using a Monte Carlo (MC) procedure. Monte Carlo profiles are grey with high transparency to visually show density. Profiles considered to be in the core of the crystal are shown in red; those in the interior are shown in yellow; and those in the rim appear in blue.

1000 µs/pixel, which result in total collection times of ~15 min per image (1024 × 1024 pixels). Contrast and brightness parameters are adjusted to maximize the difference in grayscale between the various zones within the quartz crystals. The field of view is chosen to capture each whole crystal, resulting in image resolution in the range of 1.07 to 2.74 µm/pixel (i.e. image widths of 1100 to 2800 µm: see Supplementary Material 1). The minimum resolvable timescale given our spatial resolution (spot size ~2000 nm) is approximately 10 years for $D_{Ti}^{Cherniak}$, 700 years for $D_{Ti}^{Audétat23}$, and 12,000 years for $D_{Ti}^{Jollands}$ [Bradshaw and Kent 2017].

2.2 CL Profiles

We use image processing routines written in the programming language IDL (i.e. `'cl_profile'`; see Gualda et al. [2012a]) to

extract profiles of CL intensity as a function of position from the CL images. We follow the procedures of Gualda et al. [2012a] and Gualda and Sutton [2016], and select profiles that are perpendicular to the CL zone boundary of interest (Figure 3). We strive to obtain profiles that display approximately constant CL intensity away from the boundary of interest, consistent with the boundary conditions used in the calculation of diffusion relaxation times (see below; also, Gualda et al. [2012a]). We chose to study an average of four different CL zone boundaries per quartz crystal (depending on availability), so as to obtain a series of Ti-in-quartz times, spanning from core to rim of each crystal (see Figure 2). We selected a total of 411 zone boundaries from the 93 quartz crystals (see Supplementary Material 1).

For each individual profile manually drawn across a zone boundary, `'cl_profile'` also selects five parallel adjacent profiles on either side of the selected profile, for a total of 11 profiles (Figure 3); it then calculates an 'average profile' using the mean of each corresponding point of the 11 profiles (see Figure 3B; also Gualda and Sutton [2016]). The approach here differs from that used in Gualda et al. [2012a] and Gualda and Sutton [2016] in that we use a Monte Carlo (MC) approach to better estimate uncertainties associated with the derived diffusion relaxation times. This Monte Carlo code is written by us in `Excel VBA` (Visual Basic for Applications). The Monte Carlo runs as follows: for each set of 11 parallel profiles, we generate 200 synthetic profiles assuming a Gaussian distribution centered around the observed average and standard deviation for each point in the profile (Figure 4B). We fit each of the 200 profiles to a complementary error function [Gualda et al. 2012a, see below] to calculate a set of 200 diffusion model times—one for each profile. We report the mean and the 95 % confidence interval around the mean for the resulting diffusion time; this procedure yields a better distribution of estimated diffusion times and the associated uncertainties (as opposed to using statistical measures like standard deviation), which is particularly important given that the resulting distributions tend to be skewed towards short diffusion times—diffusion time cannot be negative, but they can be infinitely long.

2.3 Calculation of maximum quartz diffusion times

We calculate the diffusional relaxation times using the equation [Crank 1979; Gualda et al. 2012a]:

$$c(x) = \frac{1}{2}\mathrm{erfc}\left(\frac{x - x_c}{2\sqrt{Dt}}\right) * [c(-\infty) - c(+\infty)] + c(+\infty) \quad (1)$$

where c is concentration, x is distance, D is the diffusion coefficient (D_{Ti}), t is time, and erfc is the complementary error function; the length scale of diffusion L equals $2\sqrt{Dt}$. This equation assumes an initial stepwise function across the boundary between two zones—this implicitly assumes that melt composition (or crystallization conditions) changes instantaneously during crystal growth, and any observed departure from a step function is attributed to post-crystallization diffusional relaxation rather than melt evolution during crystal growth. Consequentially, this means that the times derived using Equation 1 are maximum estimates [Gualda et al. 2012a; Till et al. 2015].

To optimize comparability, we use the same temperature conditions as those employed by Lubbers et al. [2022] for estimation of plagioclase diffusion times (i.e. 750 °C). This temperature is derived from the change in crystal contents and viscosity of a silicic magma with temperature, to give maximum crystal residence time under magmatic conditions while still allowing for mobilization and eruption [Cooper and Kent 2014; Bradshaw and Kent 2017; Lubbers et al. 2022; Schlieder et al. 2022]. We realize that the actual temperatures experienced by these samples could differ and evolution is likely not isothermal. While uncertainties on temperatures and thermal histories can lead to significant uncertainties in absolute diffusion times, most of our evaluations rely on relative comparisons (e.g. plagioclase versus quartz times, core versus rim zone boundaries) and crystals likely experienced very similar or identical thermal histories (derived from the same samples), such that the influence of absolute temperature and thermal history on our final results should be minimal. It is important to note that in choosing 750 °C for the reasons above, we are applying the Jollands et al. [2020] coefficient outside of their experimental range (900–1490 °C) (Figure 1). However, quartz-bearing rhyolites typically crystallize at temperatures below the conditions used in the experiments, so application is inevitably going to take place outside the calibration range (see, for instance, applications in Jollands et al. [2020]).

With the assumptions outlined above, we obtain one dataset of quartz diffusion times using $D_{\mathrm{Ti}}^{\mathrm{Cherniak}}$, one set using $D_{\mathrm{Ti}}^{\mathrm{Audétat23}}$, and one set using $D_{\mathrm{Ti}}^{\mathrm{Jollands}}$. Statistical tests for significance of differences between calculated quartz and plagioclase diffusion times are performed using `MATLAB` code, employing the `'ranksum'` function for a Mann-Whitney U-Test and a Kolmogorov-Smirnov Test.

2.4 Estimation of minimum growth rates

We calculate minimum quartz growth rates using:

$$\text{Growth rate} = \frac{d}{t} \quad (2)$$

where d is the distance from the diffusion boundary to the rim of the crystal (Figure 2 and Figure 3), and t is the calculated diffusion time for a given D_{Ti} [see Gualda et al. 2012a; Pamukçu et al. 2015; Gualda and Sutton 2016]. Distances are measured from the CL images using `IDL` routines written by us (i.e. `'cl_distance'`); we measure the distance perpendicular to the boundary of interest to the nearest crystal rim seen in the CL image (Figure 3) (Gualda and Sutton [2016]; following Pamukçu et al. [2015]). As some of the crystals are broken and some show evidence of dissolution boundaries, it can be difficult to measure the true distance to the rim of the crystal—this renders our measured distances as minimum distances. The use of minimum growth distances and maximum diffusion times implies that our growth rates are minimum estimates. Just as we calculate three sets of Ti-in-quartz diffusion times using $D_{\mathrm{Ti}}^{\mathrm{Cherniak}}$, $D_{\mathrm{Ti}}^{\mathrm{Audétat23}}$, and $D_{\mathrm{Ti}}^{\mathrm{Jollands}}$, we calculate three sets of quartz growth rates from the three D_{Ti}. This then allows us to compare each resultant set of quartz growth rates to other independent determinations of quartz growth rates [e.g. Pamukçu et al. 2015] to see which agrees best.

3 Results

3.1 Diffusional relaxation times

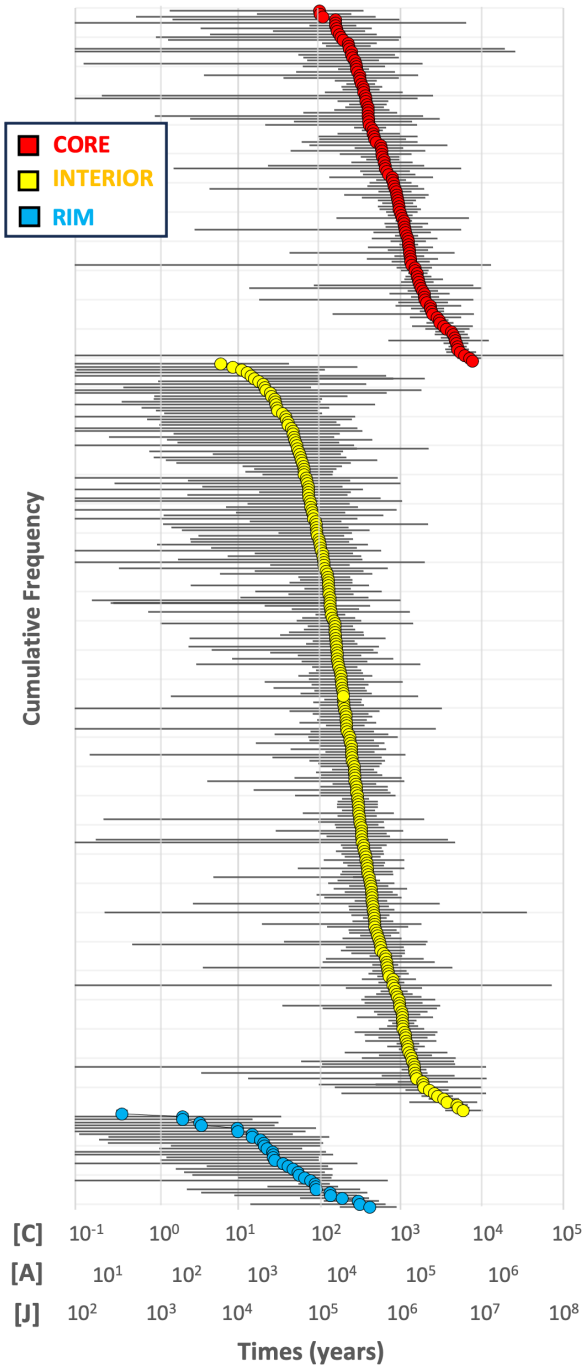

Figure 5: Calculated Ti-in-quartz diffusion timescales. Rank order diagram of diffusion times, split between core (red), interior (yellow), and rim (blue). Error bars represent a 95 % confidence interval around the mean. Three separate x-axes are given for each diffusion coefficient: Cherniak et al. [2007] (**[C]**), Audétat et al. [2023] (**[A]**), and Jollands et al. [2020] (**[J]**). Note that the **[A]** and **[J]** axes are slightly displaced from the **[C]** axis as $D_{Ti}^{Audétat23}$ is 70× larger than $D_{Ti}^{Cherniak}$, and $D_{Ti}^{Jollands}$ is 1203× larger.

Quartz diffusion times calculated using $D_{Ti}^{Cherniak}$ present a mode on the order of 10^2 years, with a range from 10^{-1} to 10^4 years (Figure 5 and Figure 6). Diffusion relaxation times generally increase from 10^{-1}–10^3 years for rim zone boundaries (blue in figures) to 10^0–10^4 years for interior boundaries (yellow) to 10^2–10^4 years for core zone boundaries (red).

Diffusion times calculated using $D_{Ti}^{Audétat23}$ are 70 times larger than $D_{Ti}^{Cherniak}$ times, presenting a mode on the order of 10^4 years, with a range from 10^1–10^6: 10^1–10^5 years for rim; 10^2–10^6 years for interior; 10^4–10^6 years for core zone boundaries.

Diffusion times calculated using $D_{Ti}^{Jollands}$ are 1203 times larger than $D_{Ti}^{Cherniak}$ times and 17 times larger than $D_{Ti}^{Audétat23}$ times, presenting a mode on the order of 10^5 years, with a range from 10^2–10^7: 10^2–10^6 years for rim; 10^3–10^7 years for interior; 10^5–10^7 years for core zone boundaries.

Importantly, uncertainties associated with individual quartz diffusion relaxation times estimated using our Monte Carlo procedure (see Figure 5) span approximately one order of magnitude, which is smaller than the two orders of magnitude difference between $D_{Ti}^{Cherniak}$ and $D_{Ti}^{Audétat23}$ mode times, and much smaller than three orders of magnitude difference in time between times calculated using $D_{Ti}^{Cherniak}$ and $D_{Ti}^{Jollands}$ (Figure 6).

3.2 Growth rates

Quartz growth rates calculated using $D_{Ti}^{Cherniak}$ are on the order of 10^{-12} to 10^{-15} m s^{-1} (Figure 10). The growth rates derived using $D_{Ti}^{Audétat}$ growth rates are again 70 times slower, yielding a range of 10^{13}–10^{16} m s^{-1}, while $D_{Ti}^{Jollands}$ growth rates are 1203 times slower than $D_{Ti}^{Cherniak}$ and 17 times slower than $D_{Ti}^{Audétat}$, yielding a range of 10^{-15} to 10^{-18} m s^{-1}.

4 Discussion

We use the results above for quartz diffusion relaxation times and growth rates in the Cerro Galán Ignimbrite to discuss three main issues: (1) comparison with Mg- and Sr-in-plagioclase diffusion relaxation times from the same samples; (2) evidence for diffusion relaxation in quartz; and (3) comparison with independently constrained quartz growth rates.

4.1 (1) Comparison with plagioclase diffusion times

Phase relationships in quartz-feldspar systems [Tuttle and Bowen 1958; Johannes and Holtz 1996; Gualda et al. 2012b; Gualda and Ghiorso 2013] reveal that quartz is never the first felsic phase to saturate in rhyolite magmas, with one feldspar always preceding quartz [see Gualda and Ghiorso 2013]. Lubbers et al. [2022] show strong evidence that plagioclase saturated prior to sanidine in Cerro Galán Ignimbrite magmas, which implies that quartz saturated after plagioclase. We thus expect that quartz diffusion times should be, on average, shorter than plagioclase diffusion times (or similar considering the errors associated with the methods used), particularly when calculated using the same diffusion conditions.

Lubbers et al. [2022] present Mg- and Sr-in-plagioclase diffusion relaxation times from the Cerro Galán Ignimbrite, and

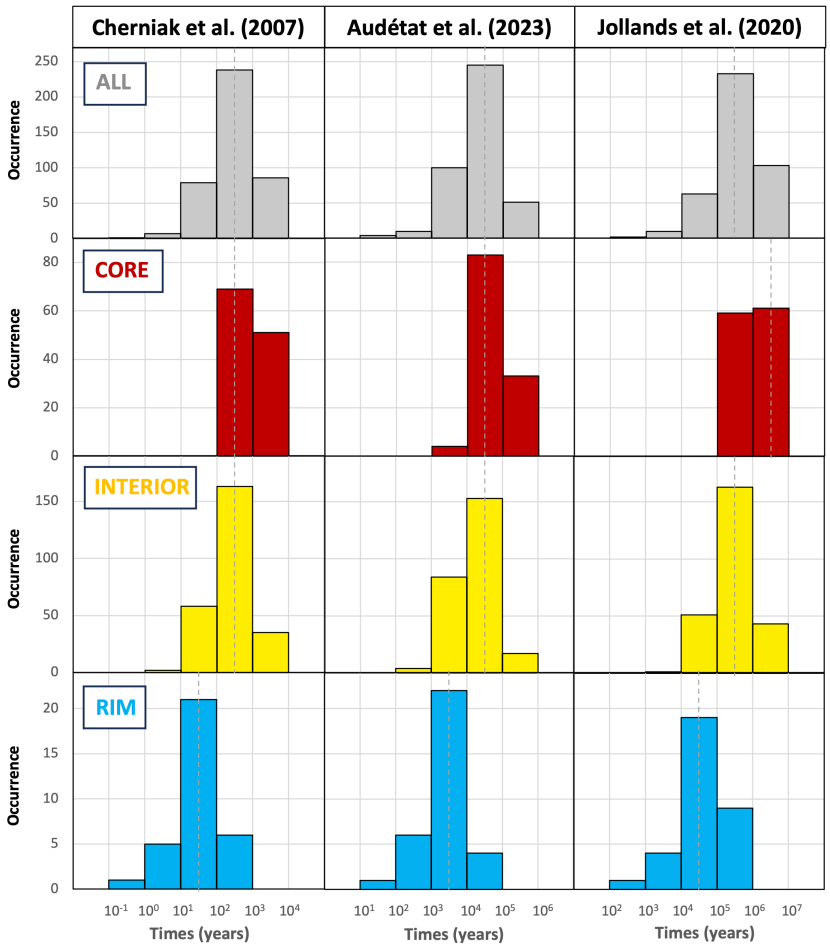

Figure 6: Comparative histograms of Ti-in-quartz diffusion times using the Cherniak et al. [2007], Audétat et al. [2023], and Jollands et al. [2020] coefficients. Histograms of all timescales shown in grey, and subdivided into core (red), interior (yellow), and rim (blue). Modes are emphasized with grey dashed lines.

they conclude that diffusion times of plagioclase calculated at 750 °C fall in the range of 10^0–10^3 years, with a mode on the order of 10^1 years (Figure 7). Comparison of the results for plagioclase from Lubbers et al. [2022] with the results for quartz obtained here show much better agreement with the results obtained using $D_{Ti}^{Cherniak}$. In all regions, times estimated using $D_{Ti}^{Cherniak}$ stand approximately one order of magnitude greater than the plagioclase times, while the times estimated using $D_{Ti}^{Audétat23}$ stand three orders of magnitude greater, and $D_{Ti}^{Jollands}$ stand four orders of magnitude greater. Most significantly, for times estimated from the outermost rim, $D_{Ti}^{Cherniak}$ times have the same mode as the plagioclase times of around 10^1 years, while the $D_{Ti}^{Audétat23}$ and $D_{Ti}^{Jollands}$ times are respectively 2 and 3 orders of magnitude greater, ~$10^{3–4}$ years (Figure 7B). Whereas quartz and feldspar cores and interiors may have experienced more variation in their pre-eruptive history, the rims of quartz and feldspar are expected to record the same final changes prior to their simultaneous eruption.

To test the similarity of distributions between chronometers, we used Mann-Whitney (MW) and Kolmogorov-Smirnov (KS) tests to compare all diffusion times as well as times from each grain region (Figure 8). Importantly, this test is nonparametric and does not require compared distributions to be normal. Typical thresholds for significance (similarity) are indicated by a p-value < 0.05. Overall distributions from all three coefficients yield p-values smaller than 10^{-4}, likely due to the wide range of our times spanning several orders of magnitude. Nonetheless, we note that rim section comparisons between $D_{Ti}^{Cherniak}$ times and the plagioclase times yield p-values of 0.1 for both tests, showing similarity between the distributions. The tests between $D_{Ti}^{Audétat23}$ and $D_{Ti}^{Jollands}$ times against plagioclase rim times yield p-values that are $\ll 0.001$ (~10^{-9} for the MW test and ~10^{-11} for the KS test), demonstrating significant dissimilarity. This again suggests that the agreement between times calculated with $D_{Ti}^{Cherniak}$ and Mg- and Sr-in-plagioclase times is greater than when compared to $D_{Ti}^{Audétat}$ and $D_{Ti}^{Jollands}$ times.

Calculation of Mg-in-plagioclase times is dependent on models of partitioning of Mg-in-plagioclase [Lubbers et al. 2022]. Recent work [Mutch et al. 2022] suggests there are complexities in the partitioning that could add additional uncertainty to the calculated times of Mg-in-plagioclase. While we acknowledge that there are uncertainties in our detailed un-

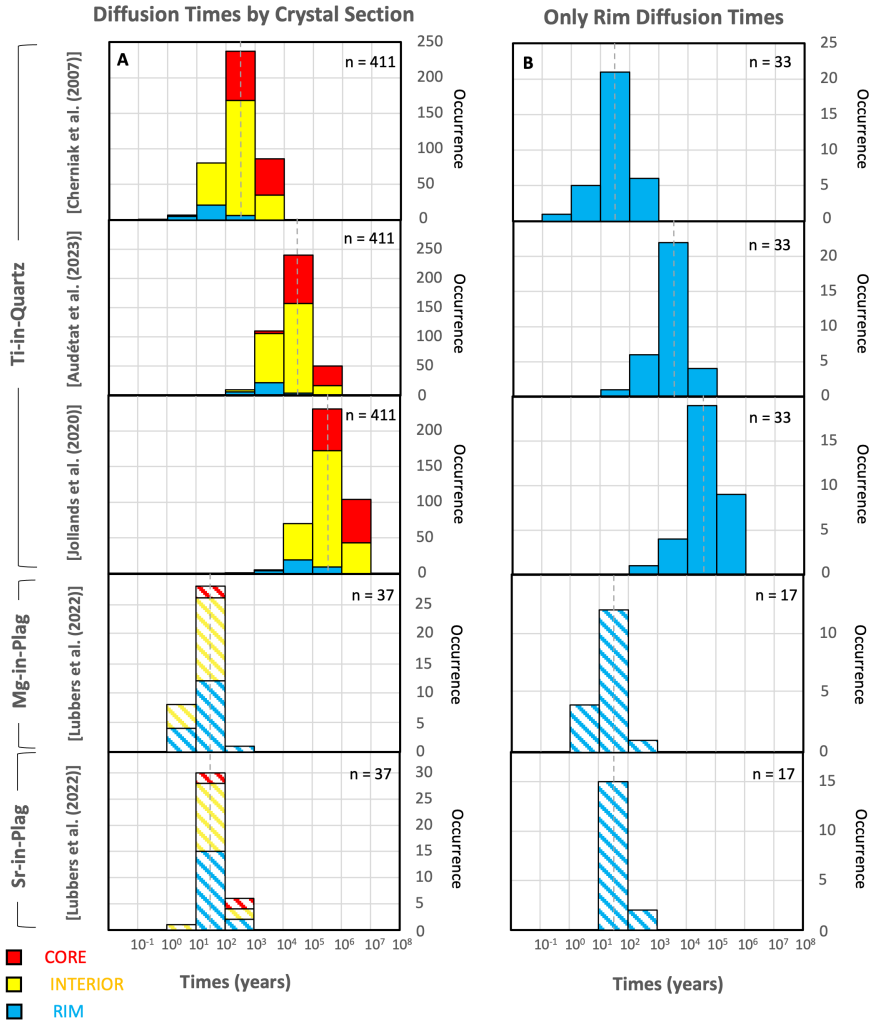

Figure 7: Comparative histograms of quartz and plagioclase timescales. Ti-in-quartz diffusion timescales using the Cherniak et al. [2007], Audétat et al. [2023], and Jollands et al. [2020] coefficient presented in solid color. Mg- and Sr-in-plagioclase diffusion timescales by Lubbers et al. [2022] presented below by striped colors. [A] Diffusion times from all crystal sections as a stacked bar graph; [B] comparison of rim times. Core timescales in red, interior in yellow, and rim in blue. Modes are emphasised with a grey dashed lined.

derstanding of Mg diffusion in plagioclase, we note that the rate with which Mg diffuses within plagioclase is sufficiently fast that Mg would relax to equilibrium profiles in roughly 10^3 years at 750 °C [Lubbers et al. 2022]. Similarly, Sr profiles would equilibrate in less than 10^5 years at 750 °C. Importantly, while Bradshaw (2017) found a few crystals in Cerro Galán Ignimbrite that are unzoned in Sr, no such crystals were found in the Lubbers et al. [2022] sample set (and, by consequence, in the samples used in this study), and the Sr profiles in plagioclase are demonstrably not in equilibrium [see Lubbers et al. 2022]. We thus conclude that plagioclase diffusion relaxation times are very likely $<10^3$ years, and definitely $<10^5$ years. Lubbers et al. [2022] also provide evidence that plagioclase initially crystallized in the absence of sanidine, but later on co-crystallized with sanidine, consistent with our inference that plagioclase was the first felsic phase to saturate in Cerro Galán magmas. Consequently, we conclude that Cerro Galán Ignimbrite quartz cannot have existed for longer than 10^5 years.

The Jollands et al. [2020] diffusion coefficient stands one order of magnitude longer than what is permissible from the plagioclase time calculations, and three orders of magnitude longer than the likely Sr-in-plagioclase equilibration times (Figure 7). In this sense, $D_{\mathrm{Ti}}^{\mathrm{Jollands}}$ is unviable for natural samples as quartz would have had to reside at magmatic temperatures up to 10^6 years before plagioclase crystallization. Times calculated using $D_{\mathrm{Ti}}^{\mathrm{Audétat23}}$ do sit within the permissible time range of the disequilibrium plagioclase. However, they stand at least two orders of magnitude greater than what is expected from our plagioclase diffusion timescales. This suggests that although $D_{\mathrm{Ti}}^{\mathrm{Audétat23}}$ provides plausible timescales in this assessment, $D_{\mathrm{Ti}}^{\mathrm{Cherniak}}$ appears the most appropriate for natural magmatic systems.

Interestingly, quartz diffusion times estimated using $D_{\mathrm{Ti}}^{\mathrm{Cherniak}}$, $D_{\mathrm{Ti}}^{\mathrm{Audétat23}}$, and $D_{\mathrm{Ti}}^{\mathrm{Jollands}}$ are longer than the plagioclase diffusion times [Lubbers et al. 2022] by one, three, and four orders of magnitude, respectively (Figure 7). As pla-

Similar — Not Similar

All	Cherniak	Audétat	Jollands	Mg
Audétat	3.5E-124			
Jollands	3.3E-135	3.4E-95		
Mg	8.2E-19	8.1E-24	6.8E-24	
Sr	1.1E-12	1.1E-23	6.8E-24	3.0E-06

Core	Cherniak	Audétat	Jollands	Mg
Audétat	7.7E-41			
Jollands	7.1E-41	2.6E-37		
Mg	7.1E-04	7.1E-04	7.1E-04	
Sr	1.6E-02	1.6E-02	1.6E-02	1.3E-01

Interior	Cherniak	Audétat	Jollands	Mg
Audétat	2.1E-83			
Jollands	5.5E-86	3.0E-69		
Mg	4.5E-10	2.0E-11	2.0E-11	
Sr	4.9E-07	1.3E-12	1.3E-12	4.1E-04

Rim	Cherniak	Audétat	Jollands	Mg
Audétat	6.1E-11			
Jollands	3.0E-12	1.2E-08		
Mg	1.6E-01	2.0E-08	9.8E-09	
Sr	2.2E-01	8.1E-08	9.8E-09	9.8E-03

Figure 8: Mann-Whitney statistical test P-values comparing quartz timescales using all three diffusion coefficients and plagioclase timescales [Lubbers et al. 2022]. Four tables divided by profile crystal region (all, core, interior, rim). Cell background is colored on a red-green scale of p-values to help with comparison of the results.

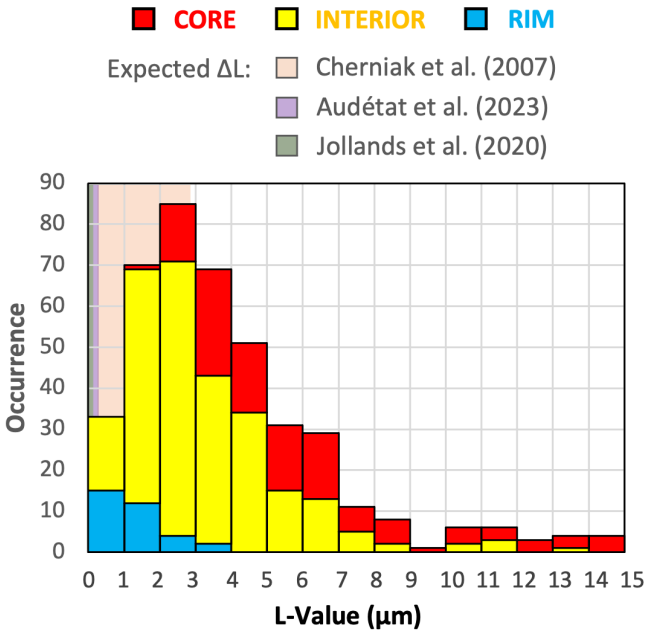

Figure 9: Histogram of measured diffusion length (L) values of profiles. L-values represent the amount of diffusion that has occurred (higher L-value indicates a smoother profile). L-values derived from core boundaries in red, interior in yellow and rim in blue. Expected diffusion (ΔL) at 750 °C over 100 years (implied by plagioclase timescales) for each Ti-in-quartz diffusion coefficient shown as orange [Cherniak et al. 2007], purple [Audétat et al. 2023], and green [Jollands et al. 2020] boxes. Note that L-values do not necessarily start at zero. Also note that L-values are generally highest for core and smallest for rim, consistent with diffusional relaxation of Ti-in-quartz, rather than resulting from growth effects.

gioclase is expected to have crystallized prior to quartz, this suggests that none of the coefficients used are perfectly accurate and the discrepancy between quartz and plagioclase diffusion times becomes larger for larger values. Even though it is unexpected that none of the coefficients gives quartz diffusion times shorter than what we observe for plagioclase, the magnitude of the difference between quartz diffusion times using $D_{Ti}^{Cherniak}$ is smaller than expected uncertainties, while quartz diffusion times calculated using $D_{Ti}^{Audétat23}$, and $D_{Ti}^{Jollands}$ are much larger, and inconsistent with the plagioclase diffusion times calculated by Lubbers et al. [2022].

4.2 Comparison with zircon crystallization times

It is generally accepted that zircon crystals, and radiometric ages of other magma phases, have much longer crystallization histories than diffusion ages recorded by quartz and plagioclase [Simon and Reid 2005; Cooper and Kent 2014; Kaiser et al. 2017], and this is typically taken to infer that much of this magmatic storage history occurred at temperatures low enough to prevent significant diffusion occurring [e.g. Cooper and Kent 2014; Lubbers et al. 2022; 2024]. U-Pb zircon ages from the Cerro Galán system [Folkes et al. 2011] show an average crystallization age of 2.35 Ma (± 0.07 Ma) from a mixture of core and rim analyses and, more importantly, a crystallization age range of 2.16–2.43 Ma, suggesting that zircon crystals crystallized over ~0.27 Myr (~10^5 years). Cerro Galán Ignimbrite quartz diffusion times using $D_{Ti}^{Cherniak}$ show shorter times (10^{-1}–10^4 years; Figure 6 and Figure 7) than the zircon crystallization times, consistent with data suggesting generally much longer age ranges for zircon when compared to quartz and suggesting long magma storage at relatively low temperatures [Lubbers et al. 2022]. Quartz diffusion times calculated using $D_{Ti}^{Audétat23}$ (10^1–10^6 years) are a closer match to zircon ages than $D_{Ti}^{Jollands}$ (10^2–10^7 years), however both reveal maximum timescales that are longer than the age span recorded by zircon. We conclude that quartz diffusion times obtained with $D_{Ti}^{Audétat23}$ and $D_{Ti}^{Jollands}$ are generally inconsistent with our understanding of mineral crystallization processes at the Cerro Galán Ignimbrite, as there is no other petrological evidence of protracted storage of other phases [Lubbers et al. 2022], while the $D_{Ti}^{Cherniak}$ yields plausible diffusion times.

4.3 (2) Evidence for diffusion relaxation

The long timescales derived from $D_{Ti}^{Audétat23}$ and $D_{Ti}^{Jollands}$ imply that the diffusion relaxation of Ti-in-quartz may be too slow to result in detectable amounts of diffusion on the decadal to millennial timeframe, the

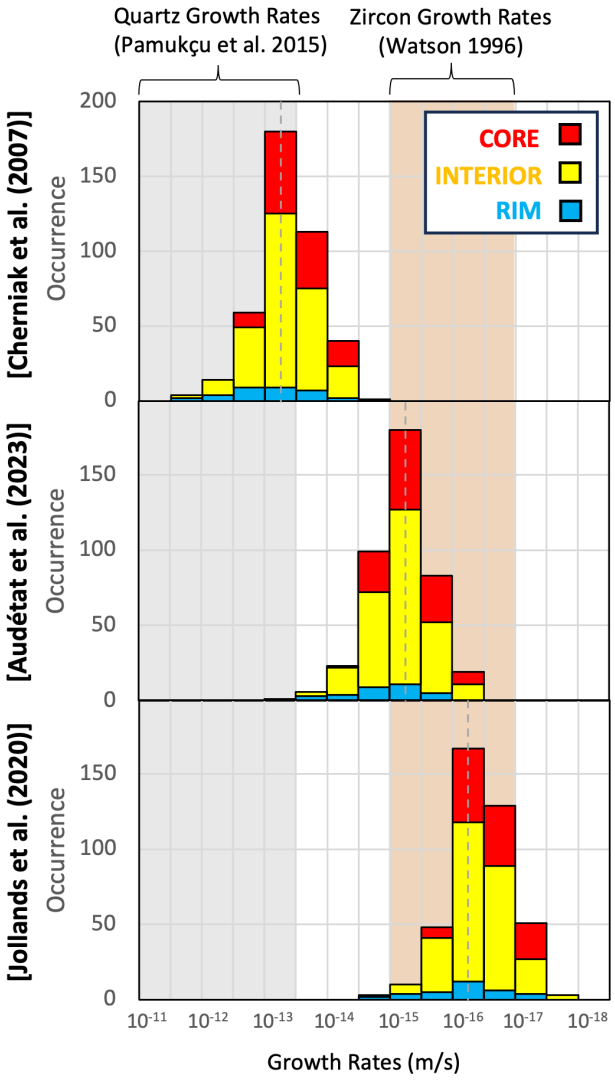

Figure 10: Histogram of calculated growth rates in $m\,s^{-1}$. Growth rates derived from a core boundary shown in red, interior in yellow and rim in blue. Values obtained using the Cherniak et al. [2007] diffusion coefficient shown on the top row, while values obtained using the Audétat et al. [2023] coefficient is on the middle row, and the Jollands et al. [2020] diffusion coefficient shown on the bottom row. For context, grey box shows expected quartz growth rates from Pamukçu et al. [2015], and brown box shows expected zircon growth rates [Watson 1996]. Modes are emphasized with a grey dashed lined.

timeframe which is commonly attributed to pre-eruptive magmatic processes [Cooper and Kent 2014; Pamukçu et al. 2015; Till et al. 2015; Shamloo and Till 2019]. If we assume diffusion at 750 °C for 100 years (as suggested by the plagioclase data), using $D_{Ti}^{Jollands}$, we calculate that a profile with an initial diffusion length (L) value of 0.20 µm would relax to 0.22 µm, remaining effectively unchanged within the resolution of our SEM condition (minimum resolution ~0.5 µm). That is to say, a quartz crystal that experienced magmatic conditions for 100 years would not exhibit any measurable change in the original diffusion gradient assuming $D_{Ti}^{Jollands}$, and all boundary profiles would display their initial crystallization profile. Similarly, using $D_{Ti}^{Audétat23}$, an initial L value of 0.20 µm would relax to 0.43 µm. In contrast, using $D_{Ti}^{Cherniak}$, a profile with initial L value of 0.20 µm would relax to a value of 3.19 µm over 100 years—in this case, changes due to diffusional relaxation would be easily measurable using our methods. Measured L-values from our quartz boundary profiles show an average diffusion length of 3.92 µm (Figure 9). This therefore strongly agrees with the rate of diffusion of $D_{Ti}^{Cherniak}$ in the given 100 years over the rate of $D_{Ti}^{Audétat23}$ or $D_{Ti}^{Jollands}$.

This conclusion relies on the assumption that the L-values measured across these boundaries were exclusively created through diffusion relaxation rather than initial growth profiles. From our results, we can see that diffusion length scales in every quartz crystal show a consistent general trend of decreasing L (diffusion length)—and hence, diffusion time—from core to rim (Figures 4, 6, 9, 11); small differences between times for similarly located boundaries fall within the expected error (~200 %; see Gualda et al. [2012a]). In other words, there is a systematic trend of quartz zone boundaries closer to the crystal core showing longer times than those closer to the rim. Given the lack of petrologic evidence for this systematic trend to be caused by melt evolution or changes in crystallization conditions, we conclude that core boundaries have relaxed by diffusion more extensively than those near the rim—this provides strong evidence that profiles themselves are the result of diffusive equilibration rather than growth [Rout et al. 2021]. We thus again conclude that diffusion of Ti-in-quartz under magmatic conditions takes place at rates much closer to $D_{Ti}^{Cherniak}$ estimates than what is suggested by $D_{Ti}^{Audétat}$ or $D_{Ti}^{Jollands}$ as they would display much smaller amounts of diffusion over 100s to 1000s of years. This conclusion is consistent with our conclusion above based on the comparison of quartz and plagioclase diffusion times.

4.4 (3) Implications for pre-eruptive crystal growth rates

The vastly different diffusion times obtained with $D_{Ti}^{Cherniak}$, $D_{Ti}^{Audétat23}$ and $D_{Ti}^{Jollands}$ have important implications for crystal growth rates under magmatic conditions. Growth rates determined experimentally vary by many orders of magnitude (~10^{-9}–10^{-12} $m\,s^{-1}$ as a minimum for skeletal and dendritic quartz morphologies), being a strong function of degree of supersaturation—usually expressed in terms of undercooling [e.g. Swanson 1977; Pamukçu et al. 2016; Barbee et al. 2020]. Hence, determination of growth rates relevant for magmatic processes has been difficult to attain. However, quartz melt inclusion faceting timescales (independent of Ti-in-quartz diffusion) suggest quartz growth rates ranging from 10^{-11}–$10^{-13.5}$ $m\,s^{-1}$ [Pamukçu et al. 2015]. For other mineral phases, Cashman [1988] uses crystal size distributions of Mount St. Helens rocks to constrain pre-eruptive plagioclase growth rates to be ~10^{-13} and 10^{-14} $m\,s^{-1}$, which are similar to the growth rates estimated by Davidson et al. [2001] for alkali feldspar. Chambers et al. [2020] date zircon inclusions within alkali feldspar, and their results suggest alkali feldspar growth rates of ~10^{-14} and 10^{-15} $m\,s^{-1}$. Importantly, Watson [1996] concludes that zircon growth rates are on the or-

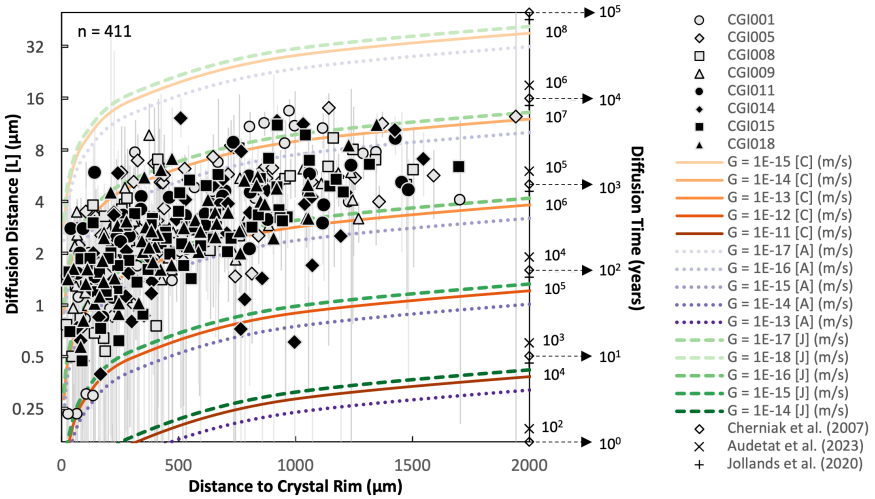

Figure 11: Summary figure showing diffusion length (*L*), Ti-in-quartz diffusion times and growth rates versus distance between the boundary of interest and the edge of the crystal for all boundaries studied here. *L*-values are shown on left vertical axis, diffusion times are shown on right vertical axis where diamond symbology represents Cherniak et al. [2007] times, crosses represent Audétat et al. [2023] times, and pluses represent Jollands et al. [2020] times. Each point represents information from a boundary profile. Samples are outlined to show there is no systematic pattern for individual samples. Error bars correspond to 95 % confidence interval. Color curves show constant growth rates, labelled **[C]** (orange), **[A]** (purple), and **[J]** (green) respectively. Note that growth rates are on a log-scale hence they appear non-linear on the diagram.

der of 10^{-15}–10^{-17} m s^{-1}. Given that zircon typically has longer crystallization histories than quartz and plagioclase (see above), and typical zircon crystals are ubiquitously 1–2 orders of magnitude smaller than typical quartz and feldspar crystals in volcanic rocks, it follows that growth rates of quartz and feldspar should be significantly faster than zircon growth rates, in order to explain the textures of volcanic rocks, including pumice from the Cerro Galán Ignimbrite.

Growth rates of quartz obtained with $D_{Ti}^{Cherniak}$ are on the order of 10^{-12} to 10^{-15} m s^{-1}, with a mode at 10^{-13} m s^{-1} (Figures 10 and 11), while growth rates using $D_{Ti}^{Audétat23}$ stand on the order of 10^{-13} to 10^{-16} m s^{-1} (10^{-15} m s^{-1} mode) and $D_{Ti}^{Jollands}$ are 10^{-15} to 10^{-18} m s^{-1} (10^{-16} m s^{-1} mode). In this sense, $D_{Ti}^{Cherniak}$ calculations are most consistent with independently determined crystal growth rates for quartz (and plagioclase) in volcanic rocks. Growth rates from $D_{Ti}^{Audétat23}$ are more plausible than $D_{Ti}^{Jollands}$, however still stand at least one order of magnitude higher than $D_{Ti}^{Cherniak}$ when compared to independently estimated growth rates.

5 Implications

This study has focused on assessing whether $D_{Ti}^{Cherniak}$, $D_{Ti}^{Audétat23}$, or $D_{Ti}^{Jollands}$ is more appropriate for Ti-in-quartz geochronometry of volcanic systems. While it is important to recognize that precision and accuracy of diffusion geochronometry of quartz and plagioclase is limited by analytical limitations [e.g. Bradshaw and Kent 2017] as well as the quality of the diffusion coefficients used, it is also important to place the results of Ti-in-quartz in the broader context of our understanding of the timescales of magmatic evolution.

In this work, we provide direct comparisons between diffusion chronometry based on Ti-in-quartz and Mg- and Sr-in-plagioclase, and we conclude that only $D_{Ti}^{Cherniak}$ can be reasonably reconciled with the plagioclase chronometry results, and with the evidence for differences in Ti diffusional relaxation from core to rim. $D_{Ti}^{Audétat23}$ leads to diffusion times that are generally one order of magnitude too long and growth rates that are one order of magnitude too slow when compared to expectations based on plagioclase (and zircon) crystallization times and experimental growth rates. Results using $D_{Ti}^{Jollands}$ differ by more than three orders of magnitude, and we thus conclude that they are implausible estimates of magmatic processes. As emphasized by Gualda and Pamukçu [2020], quartz geochronometry using melt-inclusion faceting [Gualda et al. 2012a; Pamukçu et al. 2015] leads to similar results as the results obtained here using the Cherniak et al. [2007] diffusion coefficient, reinforcing the conclusions obtained here for the Cerro Galán Ignimbrite. Similar conclusions can be drawn from comparison of diffusion geochronometry and U-series geochronology of feldspars [Cooper and Kent 2014]—uncertainties associated with the diffusivities of Mg- and Sr-in-plagioclase discussed above notwithstanding, absolute ages of plagioclase indicate a maximum average ages of plagioclase in silicic magmas of tens of thousands of years, which is inconsistent with the very long diffusion times predicted by $D_{Ti}^{Jollands}$, lending further support for the conclusions drawn here.

We recognize that recent work by Grocolas et al. [2025] has put the Sr-in-plagioclase diffusion coefficient into question, concluding Sr diffusion rates that are ~1.5–2 times slower than previously estimated [Giletti and Casserly 1994]. In the case of the Cerro Galán Ignimbrite, there is strong evidence for Ti-in-quartz diffusion relaxation (Figure 9) and Mg- and Sr-in-plagioclase diffusion relaxation where profiles have not yet reached equilibrium [Lubbers et al. 2022]. The most plausible way to achieve all these conditions simultaneously is by

using the Cherniak et al. [2007] Ti-in-quartz coefficient, the Van Orman et al. [2014] Mg-in-plagioclase coefficient, and the Giletti and Casserly [1994] Sr-in-plagioclase coefficient. We re-emphasize that we do not question the quality of the experimental studies which have provided alternate diffusion coefficients; however, these discrepancies only further emphasize the value of comparing experimental work to natural samples and vice versa.

The results obtained here, in combination with those of Lubbers et al. [2022] for feldspars, indicate that the magmas that gave rise to the Cerro Galán Ignimbrite only existed at temperatures required for it to be eruptible for decades to a few millennia, further attesting to the ephemeral nature of melt-dominated, eruption-prone magma bodies that feed very large and supereruptions, in agreement with what has been found for many other systems worldwide [Charlier et al. 2008; Gualda et al. 2012a; Matthews et al. 2012; Allan et al. 2013; Cooper and Kent 2014; Pamukçu et al. 2015; Till et al. 2015; Gualda and Sutton 2016; Seitz et al. 2016; Gualda et al. 2018; Shamloo and Till 2019; Pitcher et al. 2021; Lubbers et al. 2022].

6 Conclusions

In this work, we study in detail the CL zoning of quartz crystals from the Cerro Galán Ignimbrite, and we focus on the determination of diffusion relaxation times for Ti in quartz. We compare results obtained using the diffusion coefficients for Ti in quartz determined by Cherniak et al. [2007], Jollands et al. [2020], and Audétat et al. [2023]. We find diffusion times on the order of 10^{-1}–10^{4} years for the Cherniak et al. [2007] diffusion coefficient, with associated quartz growth rates of 10^{-12}–10^{-15} m s^{-1}; for the Audétat et al. [2023] diffusion coefficient, diffusion times are on the order of 10^{1}–10^{6} years, while growth rates are on the order of 10^{-13}–10^{16} m s^{-1}; and for the Jollands et al. [2020] diffusion coefficient, diffusion times are on the order of 10^{2}–10^{7} years, with growth rates on the order of 10^{-15}–10^{-18} m s^{-1} (Figure 11). A general trend of shorter diffusion times (smaller L-values) towards the rims of the crystals suggest that the times we calculate indeed represent diffusion relaxation and can be interpreted to yield estimates of crystal growth under magmatic conditions.

Comparison of our results with plagioclase diffusion times from Lubbers et al. [2022] reveal much better agreement between plagioclase and quartz using the Cherniak et al. [2007] diffusion coefficient than for either the Audétat et al. [2023] or Jollands et al. [2020] coefficients. The Audétat et al. [2023] coefficient agrees better than the Jollands et al. [2020] coefficient by one order of magnitude. While there are uncertainties associated with diffusion chronometry using Mg and Sr diffusion in plagioclase, times on the order of 10^{4}–10^{7} years predicted using the Jollands et al. [2020] diffusion coefficient would lead to complete re-equilibration of Mg and probably also Sr, which is demonstrably not the case for plagioclase from the Cerro Galán Ignimbrite (see Lubbers et al. [2022]).

For all these reasons, we conclude that the diffusion coefficient of Cherniak et al. [2007] is most applicable for diffusion of Ti in quartz under magmatic conditions, the Audétat et al. [2023] coefficient borders the line of permissibility, and the Jollands et al. [2020] and Audétat et al. [2021] are implausible. We do not understand the reason for the large discrepancy between the results from the various experimental studies [Cherniak et al. 2007; Jollands et al. 2020; Audétat et al. 2021], and we suggest that further experimental study of Ti diffusion in quartz is necessary. We also suggest further application of these Ti-in-quartz diffusion tests on other appropriate magmatic systems to corroborate our conclusions. For the time being, however, we recommend that the diffusion coefficient of Cherniak et al. [2007] be used in studies of Ti diffusion in quartz under natural magmatic conditions.

Our study reinforces the conclusion of prior studies that pre-eruptive quartz diffusion in silicic magmas takes place on timescales of decades to a few millennia, consistent with what is found using other minerals and geochronometry methods [Gualda et al. 2012a; Cooper and Kent 2014; Pamukçu et al. 2015; Till et al. 2015; Gualda and Sutton 2016; Gualda et al. 2018; Shamloo and Till 2019; Pitcher et al. 2021], with important implications for the timescales of evolution of silicic magmatic systems in the Earth's crust.

Author Contributions

All authors participated in the design of the project. Quartz grains were sampled and prepared by Jordan Lubbers, under supervision of Adam Kent. SEM images were taken by Guilherme Gualda. Diffusion profile analyses and diffusion times calculations were done by Sophia Wang, mentored by Guilherme Gualda. Sophia Wang led efforts to analyze data, interpret the results, and write the manuscript, in collaboration with Guilherme Gualda, Jordan Lubbers, and Adam Kent.

Acknowledgements

Special thanks to John Ayers and Calvin Miller for comments on early versions of the manuscript. This work was supported by the National Science Foundation [EAR1948862, EAR1763639] to [A.J.R.K].

Data Availability

All quartz images and selected profiles are available as Supplementary Material 1, as well as additional L-value, diffusion time and growth rate data (Supplementary Material 2). Any readers interested in the codes or additional information used in the data acquisition for this study is strongly encouraged to contact the corresponding author: Sophia Wang (sophiawang.nz@gmail.com).

Copyright Notice

References

Allan, A. S. R., D. J. Morgan, C. J. N. Wilson, and M.-A. Millet (2013). "From mush to eruption in centuries: assembly of the super-sized Oruanui magma body". *Contributions to*

Mineralogy and Petrology 166(1), pages 143–164. DOI: 10.1007/s00410-013-0869-2.

Audétat, A., N. Miyajima, D. Wiesner, and J.-N. Audinot (2021). "Confirmation of slow Ti diffusion in quartz by diffusion couple experiments and evidence from natural samples". *Geology*. DOI: 10.1130/g48785.1.

Audétat, A., A. K. Schmitt, R. Njul, M. Saalfeld, A. Borisova, and Y. Lu (2023). "New constraints on Ti diffusion in quartz and the priming of silicic volcanic eruptions". *Nature Communications* 14(1). DOI: 10.1038/s41467-023-39912-5.

Barbee, O., C. Chesner, and C. Deering (2020). "Quartz crystals in Toba rhyolites show textures symptomatic of rapid crystallization". *American Mineralogist* 105(2), pages 194–226. DOI: 10.2138/am-2020-6947.

Boro, J. R., J. A. Wolff, O. K. Neill, A. R. Steiner, and F. C. Ramos (2021). "Titanium diffusion profiles and melt inclusion chemistry and morphology in quartz from the Tshirege Member of the Bandelier Tuff". *American Mineralogist* 106(4), pages 620–632. DOI: 10.2138/am-2021-7395.

Bradshaw, R. W. and A. J. Kent (2017). "The analytical limits of modeling short diffusion timescales". *Chemical Geology* 466, pages 667–677. DOI: 10.1016/j.chemgeo.2017.07.018.

Cashman, K. V. (1988). "Crystallization of Mount St. Helens 1980?1986 dacite: A quantitative textural approach". *Bulletin of Volcanology* 50(3), pages 194–209. DOI: 10.1007/bf01079682.

Cashman, K. V., R. S. J. Sparks, and J. D. Blundy (2017). "Vertically extensive and unstable magmatic systems: A unified view of igneous processes". *Science* 355(6331). DOI: 10.1126/science.aag3055.

Chamberlain, K. J., D. J. Morgan, and C. J. N. Wilson (2014). "Timescales of mixing and mobilisation in the Bishop Tuff magma body: perspectives from diffusion chronometry". *Contributions to Mineralogy and Petrology* 168(1). DOI: 10.1007/s00410-014-1034-2.

Chambers, M., V. Memeti, M. P. Eddy, and B. Schoene (2020). "Half a million years of magmatic history recorded in a K-feldspar megacryst of the Tuolumne Intrusive Complex, California, USA". *Geology* 48(4), pages 400–404. DOI: 10.1130/g46873.1.

Charlier, B. L. A., C. J. N. Wilson, and J. P. Davidson (2008). "Rapid open-system assembly of a large silicic magma body: time-resolved evidence from cored plagioclase crystals in the Oruanui eruption deposits, New Zealand". *Contributions to Mineralogy and Petrology* 156(6), pages 799–813. DOI: 10.1007/s00410-008-0316-y.

Cherniak, D., E. Watson, and D. Wark (2007). "Ti diffusion in quartz". *Chemical Geology* 236(1–2), pages 65–74. DOI: 10.1016/j.chemgeo.2006.09.001.

Cooper, K. M. (2019). "Time scales and temperatures of crystal storage in magma reservoirs: implications for magma reservoir dynamics". *Philosophical Transactions of the Royal Society A: Mathematical, Physical and Engineering Sciences* 377(2139), page 20180009. DOI: 10.1098/rsta.2018.0009.

Cooper, K. M. and A. J. R. Kent (2014). "Rapid remobilization of magmatic crystals kept in cold storage". *Nature* 506(7489), pages 480–483. DOI: 10.1038/nature12991.

Costa, A., V. C. Smith, G. Macedonio, and N. E. Matthews (2014). "The magnitude and impact of the Youngest Toba Tuff super-eruption". *Frontiers in Earth Science* 2. DOI: 10.3389/feart.2014.00016.

Costa, F., R. Dohmen, and S. Chakraborty (2008). "Time Scales of Magmatic Processes from Modeling the Zoning Patterns of Crystals". *Reviews in Mineralogy and Geochemistry* 69(1), pages 545–594. DOI: 10.2138/rmg.2008.69.14.

Costa, F., T. Shea, and T. Ubide (2020). "Diffusion chronometry and the timescales of magmatic processes". *Nature Reviews Earth & Environment* 1(4), pages 201–214. DOI: 10.1038/s43017-020-0038-x.

Crank, J. (1979). *The mathematics of diffusion*. 2nd edition. Oxford: Oxford University Press. ISBN: 0-19-853411-6.

Davidson, J., F. Tepley, Z. Palacz, and S. Meffan-Main (2001). "Magma recharge, contamination and residence times revealed by in situ laser ablation isotopic analysis of feldspar in volcanic rocks". *Earth and Planetary Science Letters* 184(2), pages 427–442. DOI: 10.1016/s0012-821x(00)00333-2.

Fick, A. (1995). "On liquid diffusion". *Journal of Membrane Science* 100(1), pages 33–38. DOI: 10.1016/0376-7388(94)00230-v.

Folkes, C. B., S. L. de Silva, A. K. Schmitt, and R. A. Cas (2011). "A reconnaissance of U-Pb zircon ages in the Cerro Galán system, NW Argentina: Prolonged magma residence, crystal recycling, and crustal assimilation". *Journal of Volcanology and Geothermal Research* 206(3–4), pages 136–147. DOI: 10.1016/j.jvolgeores.2011.06.001.

Francis, P. W., L. O'Callaghan, G. A. Kretzschmar, R. S. Thorpe, R. S. J. Sparks, R. N. Page, R. E. de Barrio, G. Gillou, and O. E. Gonzalez (1983). "The Cerro Galan ignimbrite". *Nature* 301(5895), pages 51–53. DOI: 10.1038/301051a0.

Giletti, B. and J. Casserly (1994). "Strontium diffusion kinetics in plagioclase feldspars". *Geochimica et Cosmochimica Acta* 58(18), pages 3785–3793. DOI: 10.1016/0016-7037(94)90363-8.

Grocolas, T., E. M. Bloch, A.-S. Bouvier, and O. MÃ¼ntener (2025). "Diffusion of Sr and Ba in plagioclase: Composition and silica activity dependencies, and application to volcanic rocks". *Earth and Planetary Science Letters* 651, page 119141. DOI: 10.1016/j.epsl.2024.119141.

Gualda, G. A. R., M. S. Ghiorso, R. V. Lemons, and T. L. Carley (2012a). "Rhyolite-MELTS: a Modified Calibration of MELTS Optimized for Silica-rich, Fluid-bearing Magmatic Systems". *Journal of Petrology* 53(5), pages 875–890. DOI: 10.1093/petrology/egr080.

Gualda, G. A. R. and M. S. Ghiorso (2013). "Low-Pressure Origin of High-Silica Rhyolites and Granites". *The Journal of Geology* 121(5), pages 537–545. DOI: 10.1086/671395.

Gualda, G. A. R., D. M. Gravley, M. Connor, B. Hollmann, A. S. Pamukçu, F. Bégué, M. S. Ghiorso, and C. D. Deering (2018). "Climbing the crustal ladder: Magma storage-depth evolution during a volcanic flare-up". *Science Advances* 4(10). DOI: 10.1126/sciadv.aap7567.

Gualda, G. A. R., A. S. Pamukçu, M. S. Ghiorso, A. T. Anderson, S. R. Sutton, and M. L. Rivers (2012b). "Timescales of Quartz Crystallization and the Longevity of the Bishop Giant Magma Body". *PLoS ONE* 7(5). Edited by N. Houlie, e37492. DOI: 10.1371/journal.pone.0037492.

Gualda, G. A. R. and S. R. Sutton (2016). "The Year Leading to a Supereruption". *PLOS ONE* 11(7). Edited by A. K. Schmitt, e0159200. DOI: 10.1371/journal.pone.0159200.

Gualda, G. A. and A. S. Pamukçu (2020). "New Ti-in-quartz diffusivities reconcile natural Ti zoning with time scales and temperatures of upper crustal magma reservoirs: COMMENT". *Geology* 48(12), e513–e513. DOI: 10.1130/g48242c.1.

Jicha, B. R., D. W. Scholl, B. S. Singer, G. M. Yogodzinski, and S. M. Kay (2006). "Revised age of Aleutian Island Arc formation implies high rate of magma production". *Geology* 34(8), page 661. DOI: 10.1130/g22433.1.

Johannes, W. and F. Holtz (1996). *Petrogenesis and experimental petrology of granitic rocks*. Volume 22. Berlin: Springer Verlag. 335 pages. ISBN: 978-3-642-64671-3. DOI: 10.1007/978-3-642-61049-3.

Jollands, M. C., E. Bloch, and O. Müntener (2020). "New Ti-in-quartz diffusivities reconcile natural Ti zoning with time scales and temperatures of upper crustal magma reservoirs". *Geology* 48(7), pages 654–657. DOI: 10.1130/g47238.1.

Kaiser, J. F., S. de Silva, A. K. Schmitt, R. Economos, and M. Sunagua (2017). "Million-year melt–presence in monotonous intermediate magma for a volcanic–plutonic assemblage in the Central Andes: Contrasting histories of crystal-rich and crystal-poor super-sized silicic magmas". *Earth and Planetary Science Letters* 457, pages 73–86. DOI: 10.1016/j.epsl.2016.09.048.

Lubbers, J., A. J. R. Kent, and S. de Silva (2022). "Thermal Budgets of Magma Storage Constrained by Diffusion Chronometry: the Cerro GalÃ¡n Ignimbrite". *Journal of Petrology* 63(7). DOI: 10.1093/petrology/egac048.

– (2024). "Constraining magma storage conditions of the Toba magmatic system: a plagioclase and amphibole perspective". *Contributions to Mineralogy and Petrology* 179(2). DOI: 10.1007/s00410-023-02089-7.

Matthews, N. E., C. Huber, D. M. Pyle, and V. C. Smith (2012). "Timescales of Magma Recharge and Reactivation of Large Silicic Systems from Ti Diffusion in Quartz". *Journal of Petrology* 53(7), pages 1385–1416. DOI: 10.1093/petrology/egs020.

Morgan, D. J., S. Blake, N. W. Rogers, B. DeVivo, G. Rolandi, R. Macdonald, and C. J. Hawkesworth (2004). "Time scales of crystal residence and magma chamber volume from modelling of diffusion profiles in phenocrysts: Vesuvius 1944". *Earth and Planetary Science Letters* 222(3–4), pages 933–946. DOI: 10.1016/j.epsl.2004.03.030.

Mutch, E. J., J. Maclennan, and A. L. Madden-Nadeau (2022). "The dichotomous nature of Mg partitioning between plagioclase and melt: Implications for diffusion chronometry". *Geochimica et Cosmochimica Acta* 339, pages 173–189. DOI: 10.1016/j.gca.2022.10.035.

Pamukçu, A. S., M. S. Ghiorso, and G. A. R. Gualda (2016). "High-Ti, bright-CL rims in volcanic quartz: a result of very rapid growth". *Contributions to Mineralogy and Petrology* 171(12). DOI: 10.1007/s00410-016-1317-x.

Pamukçu, A. S., G. A. R. Gualda, F. Bégué, and D. M. Gravley (2015). "Melt inclusion shapes: Timekeepers of short-lived giant magma bodies". *Geology* 43(11), pages 947–950. DOI: 10.1130/g37021.1.

Pitcher, B. W., G. A. R. Gualda, and T. Hasegawa (2021). "Repetitive Duality of Rhyolite Compositions, Timescales, and Storage and Extraction Conditions for Pleistocene Caldera-forming Eruptions, Hokkaido, Japan". *Journal of Petrology* 62(2). DOI: 10.1093/petrology/egaa106.

Rout, S. S., M. Blum-Oeste, and G. Wörner (2021). "Long-Term Temperature Cycling in a Shallow Magma Reservoir: Insights from Sanidine Megacrysts at Taápaca Volcano, Central Andes". *Journal of Petrology* 62(9). DOI: 10.1093/petrology/egab010.

Rubin, A. E., K. M. Cooper, C. B. Till, A. J. R. Kent, F. Costa, M. Bose, D. Gravley, C. Deering, and J. Cole (2017). "Rapid cooling and cold storage in a silicic magma reservoir recorded in individual crystals". *Science* 356(6343), pages 1154–1156. DOI: 10.1126/science.aam8720.

Schlieder, T. D., K. M. Cooper, A. J. R. Kent, R. Bradshaw, and C. Huber (2022). "Thermal storage conditions and origin of compositional diversity of plagioclase crystals in magmas from the 1980 and 2004-2005 eruptions of Mount Saint Helens". *Journal of Petrology*. DOI: 10.1093/petrology/egac064.

Seitz, S., B. Putlitz, L. P. Baumgartner, S. Escrig, A. Meibom, and A.-S. Bouvier (2016). "Short magmatic residence times of quartz phenocrysts in Patagonian rhyolites associated with Gondwana breakup". *Geology* 44(1), pages 67–70. DOI: 10.1130/g37232.1.

Shamloo, H. I. and C. B. Till (2019). "Decadal transition from quiescence to supereruption: petrologic investigation of the Lava Creek Tuff, Yellowstone Caldera, WY". *Contributions to Mineralogy and Petrology* 174(4). DOI: 10.1007/s00410-019-1570-x.

Simon, J. and M. Reid (2005). "The pace of rhyolite differentiation and storage in an 'archetypical' silicic magma system, Long Valley, California". *Earth and Planetary Science Letters* 235(1–2), pages 123–140. DOI: 10.1016/j.epsl.2005.03.013.

Sparks, R., P. Francis, R. Hamer, R. Pankhurst, L. O'Callaghan, R. Thorpe, and R. Page (1985). "Ignimbrites of the Cerro Galan caldera, NW Argentina". *Journal of Volcanology and Geothermal Research* 24(3–4), pages 205–248. DOI: 10.1016/0377-0273(85)90071-x.

Spear, F. S., K. T. Ashley, L. E. Webb, and J. B. Thomas (2012). "Ti diffusion in quartz inclusions: implications for metamorphic time scales". *Contributions to Mineralogy and Petrology*. DOI: 10.1007/s00410-012-0783-z.

Swanson, S. E. (1977). "Relation of nucleation and crystal-growth rate to the development of granitic textures". *American Mineralogist* 62(9-10), pages 966–978.

Till, C. B., J. A. Vazquez, and J. W. Boyce (2015). "Months between rejuvenation and volcanic eruption at Yellowstone

caldera, Wyoming". *Geology* 43(8), pages 695–698. DOI: 10.1130/g36862.1.

Tuttle, O. F. and N. L. Bowen (1958). *Origin of Granite in the Light of Experimental Studies in the System NaAlSi3O8–KAlSi3O8–SiO2–H2O*. Geological Society of America, pages 1–146. DOI: 10.1130/mem74-p1.

Van Orman, J. A., D. J. Cherniak, and N. T. Kita (2014). "Magnesium diffusion in plagioclase: Dependence on composition, and implications for thermal resetting of the 26Al–26Mg early solar system chronometer". *Earth and Planetary Science Letters* 385, pages 79–88. DOI: 10.1016/j.epsl.2013.10.026.

Von Quadt, A., M. Erni, K. Martinek, M. Moll, I. Peytcheva, and C. A. Heinrich (2011). "Zircon crystallization and the lifetimes of ore-forming magmatic-hydrothermal systems". *Geology* 39(8), pages 731–734. DOI: 10.1130/g31966.1.

Wark, D., W. Hildreth, F. Spear, D. Cherniak, and E. Watson (2007). "Pre-eruption recharge of the Bishop magma system". *Geology* 35(3), page 235. DOI: 10.1130/g23316a.1.

Watson, E. B. (1996). "Dissolution, growth and survival of zircons during crustal fusion: kinetic principals, geological models and implications for isotopic inheritance". *Earth and Environmental Science Transactions of the Royal Society of Edinburgh* 87(1–2), pages 43–56. DOI: 10.1017/s0263593300006465.

Wilson, C. J. N. and B. L. A. Charlier (2009). "Rapid Rates of Magma Generation at Contemporaneous Magma Systems, Taupo Volcano, New Zealand: Insights from U–Th Model-age Spectra in Zircons". *Journal of Petrology* 50(5), pages 875–907. DOI: 10.1093/petrology/egp023.